Results in Physics 6 (2016) 189–193

Contents lists available at ScienceDirect

Results in Physics

journal homepage: www.journals.elsevier.com/results-in-physics

# Kerr nonlinearity enhancement by double tunnelling from quantum dot nanostructure

B. Al-Nashy [a,c], S.M.M. Ameen [a], Amin H. Al-Khursan [b,*]

[a] College of Science, University of Basrah, Basrah, Iraq
[b] Nassiriya Nanotechnology Research Laboratory (NNRL), Science College, Thi-Qar University, Nassiriya, Iraq
[c] Science College, Missan University, Missan, Iraq

ARTICLE INFO

*Article history:*
Received 21 February 2016
Accepted 4 April 2016
Available online 8 April 2016

*Keywords:*
Quantum dot
Tunnelling
Kerr dispersion

ABSTRACT

A model of the dynamical equations of the density matrix describes double tunnelling between double quantum dot (QD) system states, this is to study Kerr nonlinearity in QD structure. Inhomogeneity in the QD system is included which is not included in earlier studies of Kerr nonlinearity in QDs. Possibilities of subluminal and superluminal light propagation and switching between them are examined. Double tunnelling is shown to obtain giant Kerr dispersion compared with single tunnelling. High conduction- and low valence-band tunnelling components are required to obtain high Kerr dispersion. Working with one tunnel component reduced Kerr dispersion and switching between subluminal and superluminal can be obtained and the EIT window can be removed.



## Introduction

As is known, the Kerr nonlinearity corresponds to the real part of third-order susceptibility and has a major role in the nonlinear optics [1]. The nonlinear optical properties of an atomic medium can be modified by quantum coherence and interference too. Recent studies have shown that Kerr nonlinearity can be used for quantum non-demolition measurements, quantum bit regeneration, quantum state teleportation and the generation of the optical solitons. The quantum coherence theory such as optical bistability, electromagnetically induced transparency (EIT), superluminal light propagation without absorption and other related coherence phenomenon are studied in atomic media and in semiconductor structures in recent years [2]. To get a high Kerr nonlinearity, required for applications, low-light powers are used. This requires minimisation of absorption loss for small linear susceptibility. Conventional devices are incompatible with these requirements [3].

Due to their high nonlinearity, QDs can be used for high Kerr dispersion [2,4]. The coherence in the system can be created by coupling of two exciton states via tunnelling instead of pumping by laser beam [5]. The optical properties of quantum dots (QDs) can be substantially modified by the external field and inter-dot tunnel coupling and has found numerous implementations in semiconductor optics. Quantum dot molecules have found special attention because of their properties similar to atomic vapours, but with the advantage of flexible design and controllable interference strength [6,7]. Such a QD molecule can be fabricated using self-assembled growth technology. Enhanced Kerr nonlinearity was studied in an asymmetric GaAs double QD via Fano interference [4]. The absorption and dispersion properties of an asymmetry semiconductor double QDs system are studied and light pulse propagation is controlled using tunnel coupling [8]. A scheme for optical bistability in a tuneable three-level QD molecule formed from an asymmetry double QD system coupled by tunnelling is examined. The system interacts with a probe laser inside a unidirectional ring cavity. In this scheme, the quantum coherence is created by coupling the two exciton states via tunnelling instead of pumping laser. By suitably varying the applied voltage and laser frequency, we can realise the electrical controllability of optical bistability [3]. Villas-Boas et al., describe theoretically the behaviour of a QD-molecule formed from an asymmetric double QD system coupled by tunnelling. By applying a near resonant optical pulse they can excite one electron from the valence to the conduction band in one dot, which can in turn tunnel to the second dot [9]. Because of the tunnelling between QDs via a bias voltage, the advantage of using quantum-dots is that QDs allow direct control of its energy scales and physical properties [7].

Our aim of this work is to study the effect of double interdot tunnelling between two QDs on the nonlinear susceptibility to investigate the absorption and dispersion spectra. This is not discussed in the literatures. Note that in [10] a single tunnelling

* Corresponding author.
*E-mail address:* ameen_2all@yahoo.com (A.H. Al-Khursan).

http://dx.doi.org/10.1016/j.rinp.2016.04.003
2211-3797/

component is used which results in double EIT window. Double tunnelling components in our system are possible since the subbands of the two dots considered have near subbands for both conduction and valence bands. Additionally, inhomogeneity was not considered, yet, in the Kerr and another probing calculations in QD structures studied in the literature. These points make it critical to do this work. Our analysis is based on density matrix formalism. Our structure here has two tunnelling components and uses two controlling fields (pump and probe). A giant Kerr nonlinearity is obtained compared with other structures in studies of tunnelling in QDs. This work was organised as follows: section 2 discusses the QD susceptibility, section 3 describes the QD structure studied, section 4 states the results and its discussion. The conclusions are drawn in section 5.

## Susceptibility of QD molecule

Consider a QD molecule which is composed from the double QD system, as in Fig. 1. The subbands configuration is represented by the subband $|3\rangle$ in the conduction band and the subband $|1\rangle$ in the valence band both in the left dot, and subbands $|0\rangle$ and $|2\rangle$ in the conduction and valence bands of the right dot, respectively. The transitions $|1\rangle \leftrightarrow |3\rangle$ ($\hbar\omega_{31}$ energy) is driven by a signal field $E_s$, (frequency $\omega_s$) with Rabi frequency ($\Omega_s = E_s\mu_{31}/\hbar$(, and the transition $|0\rangle \leftrightarrow |2\rangle$ ($\hbar\omega_{20}$ energy) due to the pump field $E_p$, (frequency $\omega_p$) with Rabi frequency ($\Omega_p = E_p\mu_{21}/\hbar$(. The corresponding detuning for these transitions are $\Delta_s = \omega_{31} - \omega_s$, and $\Delta_0 = \omega_{20} - \omega_p$. The interdot tunnelling components are $T_1$ and $T_2$. Neglecting hole tunnelling is a common assumption in the literature, see for example [2,11], the total Hamiltonian of the system is

$$H_0 = \hbar[\omega_3|3\rangle\langle 3| + \omega_2|2\rangle\langle 2| + \omega_1|1\rangle\langle 1| + \omega_0|0\rangle\langle 0|] \tag{1a}$$

$$H_I = -\tfrac{\hbar}{2}[\Omega_s e^{-i\omega_s t}|3\rangle\langle 1| + \Omega_p e^{-i\omega_p t}|2\rangle\langle 0| + T_1|1\rangle\langle 0| + T_2|3\rangle\langle 2|] + h.c. \tag{1b}$$

Driving transitions between double dots by laser fields is examined in a number of works [6,10]. Our system here differs by considering double tunnelling between double QDs. Then, using the density matrix approach, we can write the following dynamical equations for our system shown in Fig. 1,

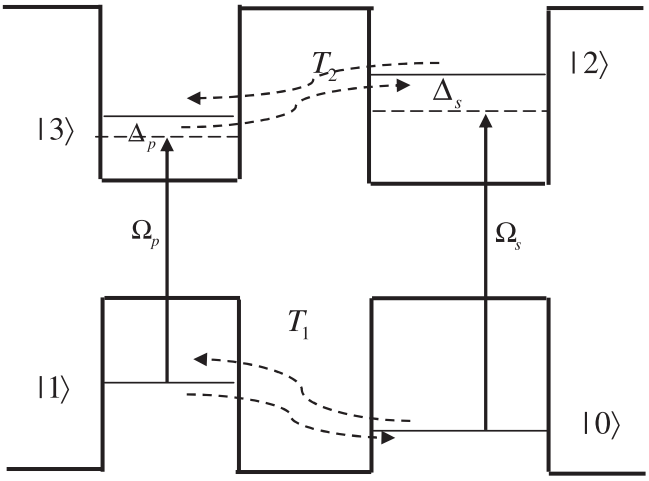


**Fig. 1.** Band diagram of the QD molecule interacting with a probe ($\Omega_s$) and pump ($\Omega_p$) fields with two tunnelling components ($T_1$) and ($T_2$). The conduction and valence subband states of the left dot are $|1\rangle$ and $|3\rangle$ while those of the right dot are $|0\rangle$ and $|2\rangle$.

$$\begin{aligned}
\rho_{00}^{(3)} &= \gamma_{20}\rho_{22}^{(3)} + iT_1(\rho_{10}^{(2)} - \rho_{01}^{(2)}) + i\Omega_p(\rho_{20}^{(2)} - \rho_{02}^{(2)})\\
\rho_{11}^{(3)} &= \gamma_{31}\rho_{33}^{(3)} + iT_1(\rho_{01}^{(2)} - \rho_{10}^{(2)}) + i\Omega_s(\rho_{31}^{(2)} - \rho_{13}^{(2)})\\
\rho_{22}^{(3)} &= -\gamma_{20}\rho_{22}^{(3)} + i\Omega_p(\rho_{02}^{(2)} - \rho_{20}^{(2)}) + iT_2(\rho_{32}^{(2)} - \rho_{23}^{(2)})\\
\rho_{33}^{(3)} &= \gamma_{31}\rho_{33}^{(3)} + i\Omega_s(\rho_{13}^{(2)} - \rho_{31}^{(2)}) + iT_2(\rho_{23}^{(2)} - \rho_{32}^{(2)})\\
\rho_{01}^{(3)} &= -[i\omega_{01} - \gamma_{01}]\rho_{01}^{(3)} + iT_1(\rho_{11}^{(2)} - \rho_{00}^{(2)}) + i\Omega_p\rho_{21}^{(2)} - i\Omega_s\rho_{03}^{(2)}\\
\rho_{20}^{(3)} &= -[i\Delta_s + \gamma_{20}]\rho_{20}^{(3)} + i\Omega_p(\rho_{00}^{(2)} - \rho_{22}^{(2)}) - iT_1\rho_{21}^{(2)} + iT_2\rho_{30}^{(2)}\\
\rho_{21}^{(3)} &= -[i\Delta_s - \gamma_{21}]\rho_{21}^{(3)} + i\Omega_p\rho_{01}^{(2)} - i\Omega_s\rho_{23}^{(2)} - iT_1\rho_{20}^{(2)} + iT_2\rho_{31}^{(2)}\\
\rho_{30}^{(3)} &= -[i\Delta_0 + \gamma_{30}]\rho_{30}^{(3)} + i\Omega_s\rho_{10}^{(2)} - iT_1\rho_{31}^{(2)} + iT_2\rho_{20}^{(2)} - i\Omega_p\rho_{32}^{(2)}\\
\rho_{31}^{(3)} &= -[i\Delta_0 + \gamma_{31}]\rho_{31}^{(3)} + i\Omega_s(\rho_{11}^{(2)} - \rho_{33}^{(2)}) - iT_1\rho_{30}^{(2)} + iT_2\rho_{21}^{(2)}\\
\rho_{32}^{(3)} &= -[i\omega_{32} + \gamma_{32}]\rho_{32}^{(3)} - i\Omega_p\rho_{30}^{(2)} + i\Omega_s\rho_{12}^{(2)} + iT_2(\rho_{22}^{(2)} - \rho_{33}^{(2)})
\end{aligned} \tag{2}$$

The relaxations ($\gamma_{ij}$) refer to the relaxation between states ($|i\rangle$) and ($\langle j|$). The third order nonlinear Kerr effect was calculated from the coherence probe transition $\rho_{20}^{(3)}$. An analytical relation is obtained by taking the solution of the system Eq. (2) at steady state. After some long mathematical manipulations following the rotten way, one can obtain the following relation

$$\begin{aligned}
\rho_{20}^{(3)} = {} & \tfrac{\Omega_p^2}{\gamma_2[i\Delta_s+\gamma_{20}]}[-i\Omega_p(\rho_{00}-\rho_{22}) + \tfrac{-T_1\Omega_p\rho_{10}+T_1\Omega_s\rho_{32}-T_1T_2\rho_{13}}{[i\Delta_s-\gamma_{21}]}\\
& + \tfrac{T_2\Omega_s\rho_{01}-T_2T_1\rho_{13}-T_2\Omega_p\rho_{23}}{[i\Delta_0+\gamma_{30}]}].d_1 - \tfrac{\Omega_p^2}{\gamma_2[i\Delta_s+\gamma_{20}]}[i\Omega_p(\rho_{00}-\rho_{22}) + d_2 + d_3].d_1\\
& - 2\tfrac{i\Omega_pT_2^2(\rho_{22}-\rho_{33})}{\gamma_2[i\omega_{32}+\gamma_{32}][i\Delta_s+\gamma_{20}]} - \tfrac{-iT_1\Omega_pT_1(\rho_{11}-\rho_{00})}{d_5[i\omega_{01}-\gamma_{01}]} + \tfrac{-iT_1\Omega_sT_2(\rho_{22}-\rho_{33})}{d_5[i\omega_{23}+\gamma_{23}]}\\
& - \tfrac{T_1^2}{d_5}[i\Omega_p(\rho_{00}-\rho_{22}) + d_2 + 2d_3].d_1 + \tfrac{-iT_1T_2\Omega_s(\rho_{11}-\rho_{33})}{d_5[i\Delta_0+\gamma_{31}]} + \tfrac{id_4\Omega_sT_1(\rho_{11}-\rho_{00})}{[i\omega_{10}-\gamma_{10}]}\\
& + \tfrac{id_4T_1\Omega_s(\rho_{11}-\rho_{33})}{[i\Delta_0+\gamma_{31}]} + T_2d_4[i\Omega_p(\rho_{00}-\rho_{22}) + d_2 + d_3].d_1 + \tfrac{iT_2d_4\Omega_p(\rho_{22}-\rho_{33})}{[i\omega_{32}+\gamma_{32}]}
\end{aligned}$$

with

$$d_1 = [(i\Delta_s + \gamma_{20}) + \frac{T_1^2}{[i\Delta_s - \gamma_{21}]} + \frac{T_2^2}{[i\Delta_0 + \gamma_{30}]}]^{-1}$$

$$d_2 = \frac{T_1\Omega_p\rho_{01} - T_1\Omega_s\rho_{23} + T_1T_2\rho_{31}}{[i\Delta_s - \gamma_{21}]}$$

$$d_3 = \frac{-T_2\Omega_s\rho_{10} + T_2T_1\rho_{31} + T_2\Omega_p\rho_{32}}{[i\Delta_0 + \gamma_{30}]}$$

$$d_4 = \frac{T_2}{[i\Delta_0 + \gamma_{30}][i\Delta_s + \gamma_{20}]}$$

$$d_5 = [i\Delta_s - \gamma_{21}][i\Delta_s + \gamma_{20}]$$

Kerr susceptibility is, then, given by,

$$\chi^{(3)}(\omega) = \frac{2N\mu_{20}^4}{3\hbar^3\varepsilon_0\Omega_s^3}\int \rho_{20}^{(3)}(\omega)D(\omega)\,d\omega \tag{3}$$

where $N$ is the atomic number density in the medium. Our formula differs from all other calculations by the inclusion of QD inhomogeneity by the convolusion over the inhomogeneous density of states which is given by [12]

$$D(E') = \frac{s^i}{V_{dot}^{eff}}\frac{1}{\sqrt{2\pi\sigma^2}}\exp\left(\frac{-(\hbar w - E_{\max}^i)^2}{2\sigma^2}\right) \tag{4}$$

$s^i$ is the degeneracy number at QD state, ($s^i = 2$) in quantum disc model used here. $\sigma$ is the spectral variance of QDs, $V_{dot}^{eff}(= h/N_D)$ is the effective volume of QDs, h is the dot height and ND is the areal density of QDs. the transition energy at the QD maximum distribution of the i$^{th}$ optical transition is $E_{\max}^i$.

## The QD structure

The proposed structure used to simulate the system shown in Fig. 1 is an asymmetric InAs double QDs with (10 nm height and 4 nm width) for the left dot and (14 nm height and 2 nm width) for the right dot. The ground conduction and valence energy subbands are (0.8 and −0.122 eV) for the left QD and (0.91 and −0.166 eV) for the right one. This structure can be obtained by the self-assemble growth technique [13]. The ground state (GS) and excited state (ES) for the left dot are the states $|1\rangle$ and $|3\rangle$ of the system, while the GS and ES of the right dot are the states $|0\rangle$ and $|2\rangle$. Since both the conduction and valence subbands of these two dots are so near, it is possible to consider tunnelling between them under a considerable gate voltage [11]. Inclusion of inhomogeneous QDs as referred above is important for susceptibility calculations. It has not been discussed before in earlier QD publications that are discussing quantum coherence and interference [7,8,10,14,15].

## Results and discussion

Throughout this work, the Kerr dispersion (third-order nonlinear susceptibility) is shown as solid red line, the nonlinear third-order absorption is shown as red dashed line, while the linear (first order) absorption (gain) is shown as blue dashed line. Also, note that the curve of linear absorption is multiplied by a factor of 50 through all the figures, for figure clarity.

Fig. 2(a) shows Kerr dispersion versus probe detuning $(\Delta_s)$ normalised to the relaxation $(\gamma_{20})$. The nonlinear third-order and the linear absorption (gain), are shown for comparison. Rabi energies for pump and probe are $(1\gamma)$ and $(0.01\gamma)$, respectively. The detuning of the pump field is $(\Delta_0 = 0.1\gamma)$. Note that all relaxations are set to $(\gamma = 1meV)$, for simplicity. High tunnelling components are used $(T_1 = 5\gamma,\ T_2 = 1\gamma)$ which is experimentally possible by applying a considerable gate voltage [6]. Many Kerr peaks are obtained at the EIT window. The Kerr peak around zero probe detuning has a positive slope and is shown corresponding to zero linear absorption but the nonlinear gain is high. So, a subluminal light propagation is expected due to this slope which is important in slow-light applications which requires large and positive dispersion [16]. Fig. 2(b) shows that reducing the second tunnelling component to $(T_2 = 0.05\gamma)$ doubles the height of the two Kerr peaks, compared with Fig. 2(a), corresponds to extreme absorption peaks of EIT. A positive slope of Kerr dispersion is obtained around $(\Delta_s = 0)$ with zero linear absorption which refers to propagation without distortion. In Fig. 2(c), reducing the first tunnelling component to the value of the second component, i.e. $(T_1 = T_2 = 0.05\gamma)$ results in a single Kerr peak that corresponds to the absorption peak. The Kerr dispersion around zero probe detuning is negative which refers to switching from subluminal to superluminal dispersion by reducing $T_1$, i.e. switching control is done by changing a single parameter. Focusing on Fig. 2(c) shows that a single peak of linear absorption is obtained without the EIT window. Trying to check results with different parameters (not appear here) shows that a high Kerr dispersion and EIT window are not obtained at low tunnelling components. This means that these low tunnelling components do not couple the dots and, then, each dot work, separately, as a single dot. Another point that must be referred to in this figure is the switching possibility of the system by control tunnelling which refers that our system is desirable for optical memory applications as a controllable variable all-optical buffer where it is possible to store and release all-optical data by controlling the tunnelling components. For all these figures, a giant Kerr is obtained compared with that obtained by other works for example, see Ref. [2]. This may result from double tunnelling components

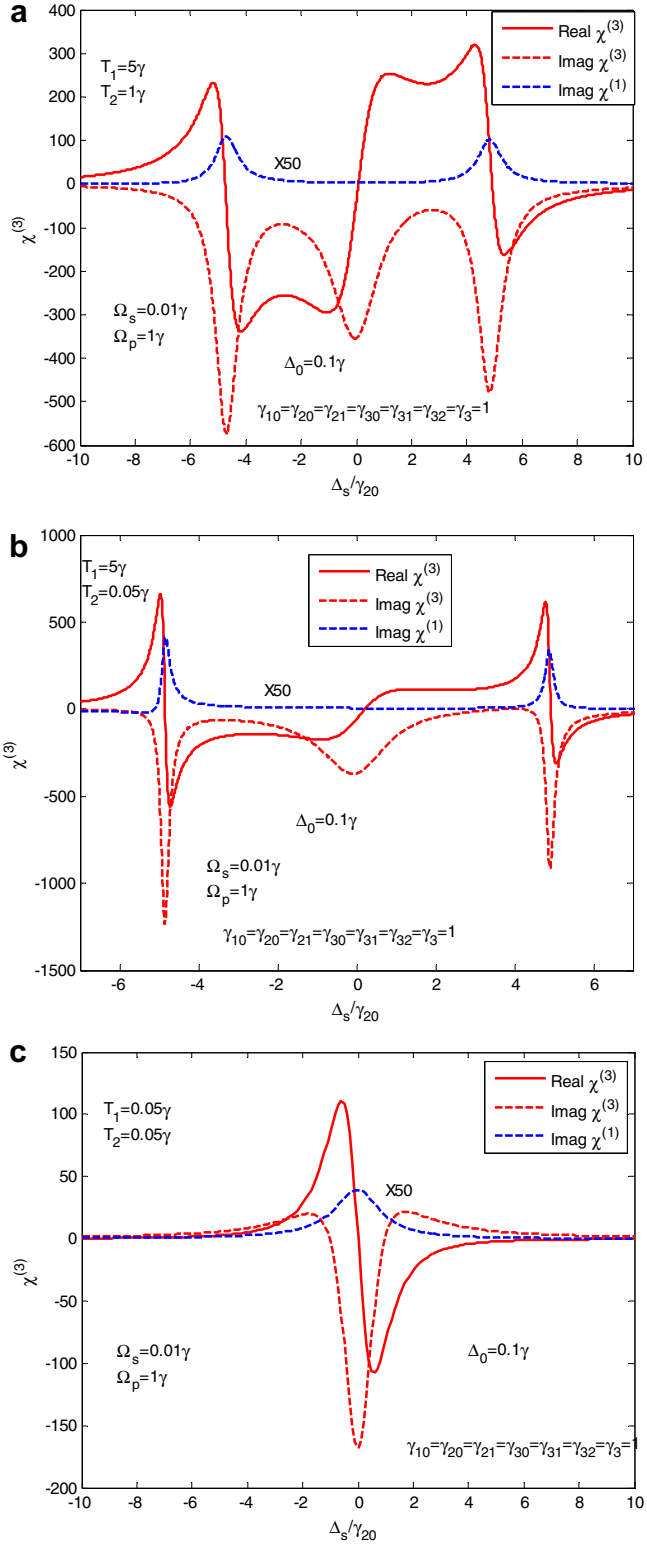


**Fig. 2.** Real "Kerr dispersion" (red solid) and imaginary (red dashed) part of third-order and linear (blue dashed) susceptibility for the QD molecule versus the probe detuning $(\Delta_s)$, normalised by its relaxation rate $(\gamma_{20})$. The Rabi frequencies for the probe field is $(\Omega_s = 0.1\gamma)$, and for the pump is $(\Omega_p = 1\gamma)$. The pump detuning is $(\Delta_0 = 0.1\gamma)$. The tunnelling components are (a) $(T_1 = 5\gamma, T_2 = 1\gamma)$, (b) $(T_1 = 5\gamma, T_2 = 0.05\gamma)$ and (c) $(T_1 = T_2 = 0.05\gamma)$. Note that the relaxations between subbands of the dots are $(\gamma_{ij} = \gamma = 1meV)$ for i,j = 1,2,3. For figure clarity, the linear susceptibility part is multiplied by (50) in all figures. (For interpretation of the references to colour in this figure legend, the reader is referred to the web version of this article.).

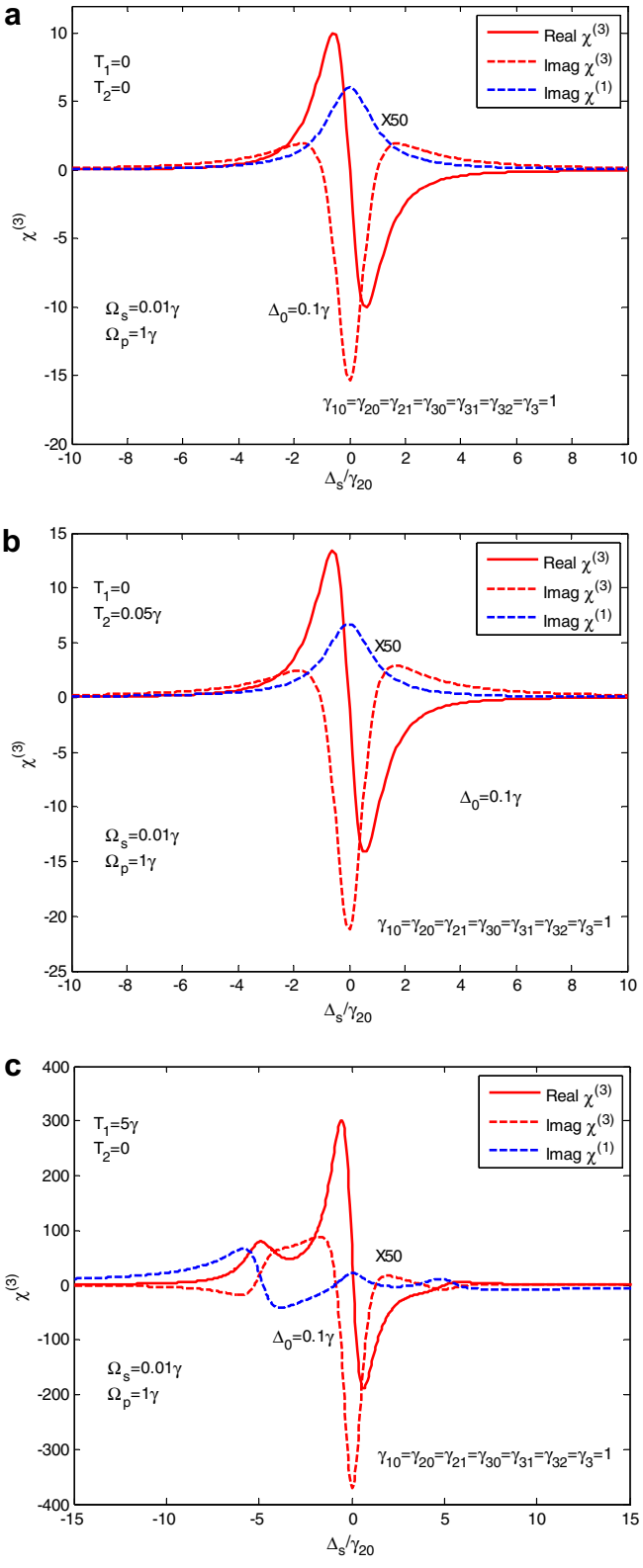


**Fig. 3.** Real "Kerr dispersion" (red solid) and imaginary (red dashed) part of third-order and linear (blue dashed) susceptibility for the QD molecule versus the normalised probe detuning. The pump detuning is ($\Delta_s = \gamma$), the Rabi frequency for the probe is ($\Omega_s = 0.01\gamma$) and for the pump is ($\Omega_p = 1\gamma$). The tunnelling components are: (a) ($T_1 = T_2 = 0$), (b) ($T_1 = 0$, $T_2 = 0.05\gamma$), (c) ($T_1 = 5\gamma$, $T_2 = 0$) and (d) ($T_1 = 0$, $T_2 = 5\gamma$). For figure clarity, the linear susceptibility part is multiplied by (50) in all figures. (For interpretation of the references to colour in this figure legend, the reader is referred to the web version of this article.).

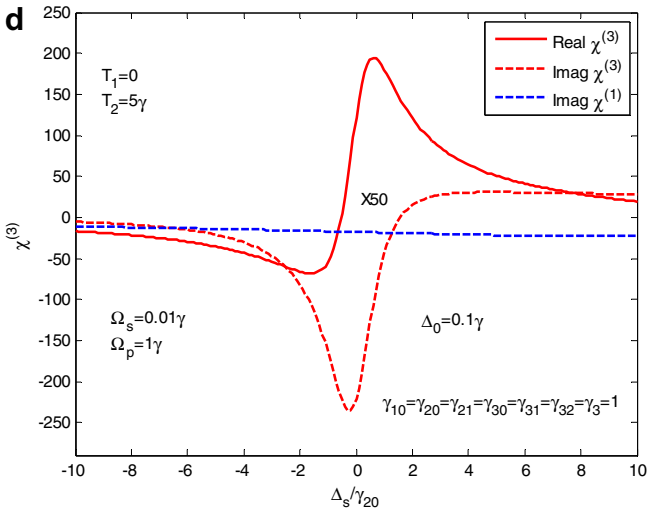


**Fig. 3** (*continued*)

used here. To check the validity of uncoupled dots at low tunnelling, Fig. 3(a) shows the case of turning off the two tunnelling components, i.e. ($T_1 = T_2 = 0$). A single Kerr peak is shown with no EIT window, a result similar to that in Fig. 2(c). The Kerr peak is reduced by more than one order of magnitude. This shows the importance of including tunnelling components. To examine the two components, Fig. 3(b) shows the case when the first tunnelling component is turned off ($T_1 = 0$). A result same as Fig. 3(a) is obtained, only the Kerr peak is somewhat higher due to the second tunnelling component where $T_2 = 0.05\gamma$. Fig. 3(c) shows the case when the second tunnelling component is turned off and high tunnelling from the first component is used, ($T_1 = 5$, $T_2 = 0$). Two EIT windows and two Kerr peaks are obtained with negative slope for the peak around zero probe detuning. Kerr peak higher (by 30 times) than that is obtained when both tunnelling components are turned off, Fig. 3(a). This is desirable for all-optical switching applications which need maximal Kerr nonlinearities [2]. Turning off the first tunnelling component, as in Fig. 3(d), switches the Kerr dispersion from negative to positive, i.e. to subluminal light dispersion with zero linear and low nonlinear absorption. The Kerr peak is high.

## Conclusions

A model for double tunnelling in the double QD system is stated using the density matrix theory where Kerr dispersion relation is obtained which is then studied and compared with linear and nonlinear absorption (gain). QD inhomogeneity is included which is not covered in earlier Kerr studies in QDs. Our system shows that light can propagate subluminal and superluminal without distortion or noise. For propagation at the middle of the EIT window high tunnelling components are required. EIT window can be removed when the tunnelling component at the valence band is removed.

## References

[1] Schmidt H, Imamoglu A. Giant Kerr nonlinearities obtained by electromagnetically induced transparency. Optics Lett 1996;21:1936–8.
[2] Asadpour SH, Sahrai M, Bonabi RS, Soltani A, Mahrami H. Enhancement of Kerr nonlinearity at long wavelength in a quantum dot nanostructure. Physica E 2011;43:1759–62.
[3] Kang H, Zhu Y. Observation of large Kerr nonlinearity at low light intensities. Phys Rev Lett 2003;91:093601.

[4] Jiang YW, Zhu KD. Controlling Kerr nonlinearity with electric fields in asymmetric double quantum-dots. Cond-Mat.Mes-Hall 2008. arXiv:0801.3726v1.
[5] Li J, Yu R, Liu J, Huanga P, Yang X. Voltage-controlled optical bistability of a tunable three-level system in a quantum-dot molecule. Physica E 2008;41:70–3.
[6] Sahrai M, Reza Mehmannavaz M, Sattari H. Optically controllable switch for light propagation based on triple coupled quantum dots. Appl Opt 2014;53:2375–83.
[7] Chang-Hasnain CJ, Ku PC, Kim J, Chuang S-L. Variable Optical Buffer Using Slow Light in Semiconductor Nanostructures. Proceedings of IEEE 2003;91:1884–97.
[8] Mahmoudi M, Sahrai M. Absorption-free super luminal light propagation in a quantum-dotmolecule. Physica E 2009;41:1772–8.
[9] Villas-Boas JM, Govorov AO, Ulloa SE. Coherent control of tunnelling in a quantum dot molecule. Phys Rev B 2004;6:125342.
[10] She Y, Zheng X, Wang D, Zhang W. Controllable double tunnelling induced transparency and solitons formation in a quantum dot molecule. Opt. Express 2013;21:17392–403.
[11] Vafafard A, Goharshenasan S, Nozari N, Mohmoudi A. Phase-dependent optical bistability in the quantum dot nanostructure molecules via inter-dot tunnelling. J Luminescence 2013;134:900–5.
[12] Bimberg D, Kirstaedter N, Ledentsov NN, Alferov ZhI, Kop'ev PS, Ustinov VM. InGaAs–GaAs Quantum-Dot Lasers. IEEE J Sel Top Quantum Electron 1997;3:196–205.
[13] Tarasov GG, Zhuchenko ZY, Lisitsa MP, Mazur YI, Wang MZ, Salamo GJ, Warming T, Bimberg D, Kissel H. Optical detection of asymmetric quantum-dot molecules in double-layer InAs/GaAs structures. Semiconductors 2006;40:79–83.
[14] Bai Y, Liu T, Yu X. Giant Kerr nonlinearity in an open V-type system with spontaneously generated coherence. Optik 2013;124:613–6.
[15] Sahrai M, Tajalli H, Kapale KT, Zubairy MS. Tunable phase control for subluminal to superluminal light propagation. Phys Rev A 2004;70:023813.
[16] Ku PC, Chang-Hasnain CJ, Chuang SL. "Slow light in semiconductor heterostructures. J Phys D Appl Phys 2007;40:R93–R107.